JOURNAL OF APPLIED POLYMER SCIENCE VOL. 17, PP. 3391–3422 (1973)

Dynamic Mechanical Properties of Some Epoxy Matrix Composites

J. R. JENNESS, JR.,* and D. E. KLINE,
Department of Material Sciences, The Pennsylvania State University, University Park, Pennsylvania 16802

Synopsis

Dynamic mechanical properties of some epoxy matrix composites have been studied, comparing experimental data with theoretical models. The matrix in all composite samples was Shell Epon 828, a diglycidyl ether of bisphenol A, cured with *meta*-phenylenediamine. Fibrous composite samples were made with glass and graphite fibers. Particulate composite samples were made with glass microspheres, atomized aluminum, powdered silica, alumina, asbestos, mica, carbon black, and graphite. The dynamic elastic modulus and damping of these samples were measured at temperatures between 85° and 345°K by a free-free flexural resonance technique. The dynamic modulus of parallel fiber composites follows the linear rule of mixtures for low fiber volume fractions; deviations from linearity at higher volume fractions appear to be due to defects caused by the sample fabrication technique. Dynamic moduli of the particulate composites conform, within experimental error, to the static modulus theory of Wu up to filler volume fractions of 0.35 to 0.40. Deviations from Wu's theory at higher volume fractions may be due to agglomeration of filler particles. The damping of particulate composites with quasi-spherical filler particles appears to follow the rule of mixtures. In particulate composites with needle- and flake-type fillers, and in fibrous composites, the fillers are more highly stressed; with more of the strain energy in the low-damping fillers, overall damping is reduced. Damping greater than that attributable to the matrix and filler may be due to slippage at the interface between them. In addition to supporting Wu's theory of the elastic modulus of a particulate composite, this study demonstrates the utility of the nondestructive free-free flexural resonance techniques for obtaining a large body of reliable data in a short time from relatively few small samples. This greatly facilitates the experimental testing of theoretical models and the evaluation of fillers, matrix materials, and fabrication techniques.

INTRODUCTION

Epoxy matrix composites are of considerable interest in composite materials research because of the desirable properties of epoxy resins and the polymer systems they form. The resins have indefinite shelf life; they have little tendency to polymerize spontaneously without curing agents. A wide variety of curing agents, curing temperatures, and curing cycles makes them suitable for a number of manufacturing processes. Other desirable properties are chemical inertness of the cured systems, low shrink-

* Present address: Scitek, Inc., State College, Pennsylvania 16801.

age on curing, curing reactions which may evolve no significant by-products, strong adhesion to other materials, and compatibility with many different fillers and additives.

The elastic modulus of a composite material depends on the moduli of the matrix and filler, and on various subtle effects of the mixing and molding techniques. Longitudinal elastic moduli of parallel fiber composites follow a simple linear law, at least for uniform tensile stresses and small strains. However, as Nielsen[1] had pointed out, the general state of theoretical models for moduli of particulate-filled composites has been unsatisfactory.

Modulus estimates have been derived from strain energy calculations, assuming equal stress and equal strain in the matrix and filler particles. The equal-stress and equal-strain estimates establish rigorous bounds for the composite modulus, but the gap between them is rather large. By a variational analysis, Hashin and Shtrikman[2] have reduced the gap to an amount acceptable for some materials, such as two-phase metal alloys, in which the moduli of the phases do not differ widely. However, for polymers filled with metallic or mineral particles the gap is still too wide to permit useful predictions of experimental results.

A number of composite modulus models are adaptations of theories of the viscosity of a liquid with solid particles in suspension. They rely on a presumed analogy between stress–strain relationships in an elastic solid and stress–strain rate relationships in a viscous liquid. Mooney's theory[3] is in fair agreement with some experimental results for particulate-filled elastomers, but its predictions are too high for composites with a rigid polymer matrix.

Another approach to the development of a composite modulus theory is to examine the stress–strain behavior of a single filler particle and the matrix material near it and generalize the result to an average for a large number of closely spaced particles. Kerner[4] has presented such a model for particles of spherical shape, which gives a conservatively low estimate of the modulus of epoxy–matrix composites. More recently, Wu[5] has developed a theory which gives an estimate higher than that of Kerner's theory but lower than that of Mooney's theory and also takes into account the effect of filler particle shapes other than spheres.

The proof of a theoretical model requires the accumulation of a large body of experimental data. Conventional static mechanical testing to destruction requires a large enough number of samples to give statistically significant data for any given condition. If conditions such as filler concentration and matrix formulation are to be varied, including temperature as a parameter, the number of specimens required becomes almost prohibitive. Fabrication and testing of large numbers of samples can be very expensive and time-consuming. Therefore, nondestructive dynamic mechanical testing is gaining acceptance as a method which supplements or complements and in many cases clearly replaces static testing techniques.

During the past twenty years, dynamic mechanical testing has gained recognition as a research method which can supplement such techniques as

chemical analysis, infrared spectroscopy, nuclear magnetic resonance, and dielectric measurements in the determination of the molecular structure of polymers. Quite a few papers on the dynamic mechanical properties (DMP) of amine-cured epoxy systems have appeared.[6-18] These studies show that such systems may have their primary glass transition temperature as high as the range in which thermal degradation begins. They also have strong secondary relaxations in the 200–300°K range, and some systems have a third relaxation below 200°K. These relaxations and their variations with molecular structures of resins and curing agents, and other factors such as heat treatment, have given insights into the structures of these polymers and processes for controlling them.

Research on the dynamic mechanical properties of epoxy-matrix composites has accelerated in the past five years. Galperin[19] studied the dynamic mechanical properties of an epoxy system filled with TiO_2 particles. Schultz and Tsai[20] studied unidirectional glass fiber composites with the fibers oriented at several different angles relative to the sample axis. Lifshitz and Rotem[21] studied powdered silica–epoxy composites, and Saxton and Kline[22] used an atomized aluminum filler. Nielsen and Lewis[23,24] worked with several particulate-filled composites. Dudek[25,26] studied unidirectional carbon fiber–epoxy composites. Hirai and Kline[27,28] investigated composites with some particulate carbon and graphite fillers.

These workers used a variety of techniques to determine the dynamic mechanical properties. A number of them employed torsion pendulums similar to that of Nielsen.[29] Others, including Schultz and Tsai[20] and Dudek,[25,26] vibrated their samples in cantilever or vibrating reed modes. The free-free flexural resonance technique of Förster[30] is one of those preferred by Kline[7] and his associates.

To date, DMP research has consisted mostly of studies of unfilled polymer systems and investigations of certain specific composites. No comprehensive presentation of the elastic moduli of composites based on a single epoxy matrix with a variety of fillers has yet appeared. The present study has as its objective an examination of the DMP of representative composites based on a matrix of a diglycidyl ether of bisphenol A cured with a stoichiometric concentration of *meta*-phenylenediamine. Measurements were made of the dynamic elastic modulus and internal friction of composite samples by the Förster method[30] using a free-free flexural resonance test system designed by Kline.[31] A selected assortment of fibrous and particulate fillers was chosen to explore the mechanical properties of composites with this matrix. Experimental data were analyzed to test the validity of Wu's theory of the elastic modulus of a particulate composite.[5]

EXPERIMENTAL

Sample Preparation

The epoxy resin used as the matrix in all composite samples was a diglycidyl ether of bisphenol A, Epon 828, a product of the Shell Chemical

Company. The supplier characterizes the molecular structure of this resin as

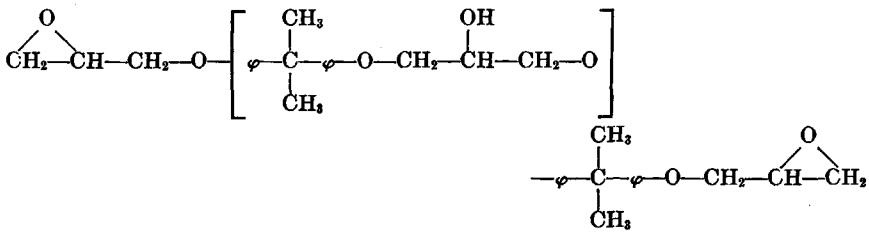

where the symbol φ represents the phenyl group of aromatic ring. For $n = 0$, the molecular weight is 340, and this species is the major constituent. Longer-chain molecules are present in sufficient concentration to make the average molecular weight 370 to 385. If $n = 1$ for all these, an average molecular weight of 370 would mean that 90% of the molecules are of the smaller species. If molecules with $n > 1$ are present, $n = 0$ for more than 90% of the population.

This resin was cured with *meta*-phenylenediamine (mPDA), with structure $H_2N—\varphi(NH_2)$ and molecular weight 108. Assuming an average molecular weight of 370 for the resin, with two epoxide groups per molecule, its epoxide equivalent is 185. Then the stoichiometric mass ratio is 14.6 parts mPDA per 100 parts of the resin.

This curing agent is a solid at room temperature, so mixing is facilitated if both it and the resin are heated to its melting point, 62.8°C. However, it was found desirable to inhibit premature polymerization by minimizing the time the mixture was kept above this temperature. A stoichiometric amount of mPDA granules was poured onto the resin and the container was placed on a low-power electrical heating element until the mPDA granules floating on the resin began to melt. At the mPDA melting temperature, the viscosity of the resin is low enough to facilitate mixing without stirring. This avoids the introduction of air bubbles which might contribute to the formation of voids in the sample. It was found that homogeneous mixing of the resin and molten mPDA (indicated by a uniform light-brown color) could be achieved within 1 to 3 minutes by a gentle rocking oscillation of the container while keeping the temperature of the mixture below 75°C. After removal from the heat, a small batch (50 g or less) cooled to room temperature in about 20 minutes.

For fibrous composite samples, rovings of Owens-Corning E glass fibers and tows of Great Lakes Fortafil 6T graphite fibers were used. (A roving is a loose yarn with a slight twist. A tow is a looser untwisted bundle of fibers.) Data on these fibers are compiled in Table I. A fiber bundle, consisting of a predetermined number of rovings or tows in parallel, was impregnated with the warm freshly prepared epoxy–mPDA mixture, then compressed in a rectangular bar mold, as shown in Figure 1.

TABLE I
Reinforcing Fibers

Fiber	Supplier	Supplier's designation	Approximate fiber diameter, μm	Density, g/cm^3	Elastic modulus, dynes/cm^2	Poisson ratio	Ultimate strength, dynes/cm^2
Glass	Owens-Corning Fiberglas Corp.	E glass	7.5	2.54	72.5×10^{10}	0.22	3.5×10^{10}
Graphite	Great Lakes Carbon Corp.	Fortafil 6T	10	1.89	400×10^{10}	0.2	2.9×10^{10}

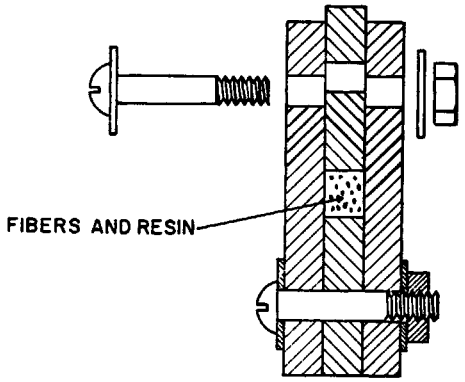

Fig. 1. Technique for molding fibrous composite samples.

Data on the fillers used in particulate composite samples are compiled in Table II. The glass microspheres and the aluminum, silica, and alumina fillers, with quasi-spherical filler particles, could be mixed into the warm resin–mPDA liquid and poured into a mold up to a volume fraction (v_f) of about 0.5. For the graphite flakes, the maximum v_f for which the mixture could be poured was about 0.3. For mica flakes and carbon black, the maximum pourable v_f was about 0.2, and for asbestos, it was only 0.12.

Immediately after mixing the resin and filler, the mixture was placed in a vacuum chamber to remove as much as possible of the air entrained by the filler particles. After collapse of the bubbles, the mixture was removed from the vacuum chamber and poured into a rectangular bar mold, as shown in Figure 2. With a glass strip for the mold cover, it was possible to detect and remove air pockets trapped during the mold closure operation.

Chopped fiber (whisker) composites, intermediate in properties between parallel fiber and particulate composites, present special problems in sample preparation. Fibers with a maximum length of 3 mm cannot be handled as long fibers in tows or rovings, but neither can they be treated as particles. With short fiber fillers, a relatively low value of v_f immobilizes the resin, so chopped fiber–resin mixtures cannot be poured as particulate composite mixtures over a very large range of v_f. This offers some explanation for the finding that the maximum pourable v_f with the asbestos filler was only 0.12; the asbestos filler particles are mostly short fibers or needles. With chopped glass fibers, the maximum pourable v_f was found to be 0.15, and it was possible to mold a rectangular bar sample with this concentration. With chopped graphite fibers, no mixture with a significant v_f could be poured, and another technique was employed.

The technique for making chopped fiber composite samples with more than the maximum pourable v_f is illustrated in Figure 3. A glass tube (coated on the inside with grease to prevent adhesion of the cured epoxy–mPDA polymer) was packed with chopped fibers and the epoxy–mPDA mixture was drawn up the tube by vacuum. Chopped graphite fibers of about 3-millimeter length (Great Lakes Fortafil 6T, identical with the long

TABLE II
Particulate Fillers

Filler	Supplier	Supplier's designation	Maximum particle diameter, μm	Density, g/cm³	Elastic modulus, 10^{10} dynes/cm²	Poisson ratio
Glass microspheres	Cataphote Corp.	3200 Uni-spheres	30	2.35	71	0.22
Atomized aluminum	Alcoa	101	30	2.52	69.6	0.33
Powdered silica	Glasrock Products, Inc.	−325 DRG Glasgrain	40	2.0	69	0.22
Powdered alumina	Alcoa	814	30	3.81	408.5 (Voigt) 391.3 (Reuss)	0.230 0.228
Mica	Diamond Mica Co.	325 water ground	60	2.82	100.8 (Voigt) 56.8 (Reuss)	0.227 0.279
Asbestos	Powhatan Mining Co.	25 PM	15	3.0	175	unknown
Natural graphite	National Carbon Co.	SP-1	60	2.10	524 (Voigt) 25 (Reuss)	0.197 0.390
Carbon black	Cabot Corp.	Regal 330 R	60	1.80	unknown	unknown

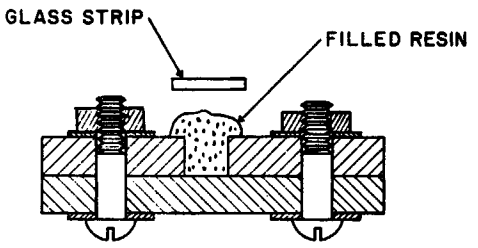

Fig. 2. Technique for molding particulate composite samples.

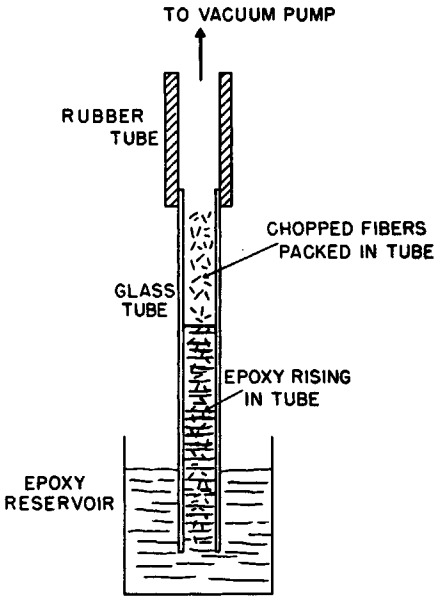

Fig. 3. Technique for molding chopped-fiber composite samples.

fibers in the parallel fiber composite samples) packed into the tube to a density sufficient to give a v_f value of only 0.046 so impeded the flow of the epoxy–mPDA mixture that 2 hr of pumping with a full atmosphere of vacuum were required to make it flow through a 12-cm tube length. With 3-mm chopped glass fibers (Owens-Corning E glass, as in the long fiber composite samples) packed into the tube by a ramrod, v_f was increased to 0.21.

After compressing a resin-impregnated fiber bundle (Fig. 1), pouring particulate-filled resin into the mold (Fig. 2), or drawing the resin into a fiber-filled tube (Fig. 3), the samples were left in their mold assemblies 18 hr to cure to a solid phase at room temperature, the first stage of a two-step cure. After this 18-hr room-temperature cure, the mold assemblies were placed in a 70°C oven for 24 hr. The heat capacity of the mold assembly in contact with the resin prevented the exothermic heat of the curing reaction from raising the sample temperature more than a fraction of a degree above the oven temperature.

To estimate the extent of the curing reaction, infrared absorption measurements were made on small fragments broken off an unfilled epoxy–mPDA sample after the initial room-temperature cure and after the final oven cure. These fragments were pulverized, mixed with KBr powder, and compressed to form thin discs for the sample holder of a Perkin-Elmer grating infrared spectrometer, Model 621. The epoxide band at 915 cm^{-1} was examined to determine the portion of the epoxide groups which had reacted after each of these curing steps. It indicated that about 60% of the epoxide groups react during the room-temperature cure. After the final 70°C oven cure, about 75% have disappeared.

After the 24-hr cure at 70°C, the mold assemblies were removed from the oven. Rectangular bar molds were dismantled to remove fibrous and particulate composite samples with cross-sectional dimensions approximately 6 mm × 5 mm. Chopped-fiber composite samples molded in glass tubes were retrieved by breaking the tubes off the outside, giving a round bar about 8 mm in diameter. All samples were trimmed to a length of about 11 cm.

The volume fraction v_f of filler in a composite is a basic parameter to which its properties are often referred. It can be shown that for a parallel fiber composite fabricated by the technique of Figure 1,

$$v_f = \frac{Nm}{\rho_f A} \tag{1}$$

where N is the number of resin-impregnated tows or rovings laid into the rectangular bar mold, m is the mass per unit length of the tow or roving, ρ_f is the density of the fibers in the tow or roving, and A is the cross-sectional area of the rectangular bar sample. For a particulate composite formed by mixing a mass M_f of filler into a mass M_m of matrix material,

$$v_f = \frac{1}{1 + \dfrac{\rho_f M_m}{\rho_m M_f}} \tag{2}$$

where ρ_f is the density of the filler and ρ_m is the density of the matrix, 1.20 g/cm^3 for the present epoxy–mPDA system. If there are no voids, the value of v_f computed by eq. (2) will be equal to

$$v_f = \frac{\rho_c - \rho_m}{\rho_f - \rho_m} \tag{3}$$

where ρ_c is the density of the composite determined from the mass and volume of the cured sample. If the sample contains voids, the volume fraction of voids is given by

$$v_v = \left[\frac{\rho_f}{\rho_m} - 1\right](v_{f2} - v_{f3}) \tag{4}$$

where v_{f2} is the value of v_f given by eq. (2) and v_{f3} is that given by eq. (3).

Vacuum pumping to remove air entrained by the spherical and quasi-spherical filler particles made the value of v_f from eq. (3) approach that predicted by eq. (2) up to 0.35 or 0.40. In the upper v_f range the spaces between the filler particles are smaller, and not all the microbubbles can escape. Asbestos whiskers and flat flake fillers (mica and graphite) caused more air retention than the quasi-spherical filler particles; the value of v_f given by eq. (3) fell below that from eq. (2) over the full range of v_f for these fillers.

Dynamic Mechanical Testing

The equipment for flexural resonance testing has been described in detail by Kline.[31] The sample is suspended in a test cell by two threads just outside the nodes of the fundamental free-free mode, as shown in Figure 4. One thread is driven at middle-audio frequencies (500–3500 Hz) by a magnetostrictive transducer. The other thread is in contact with a piezoelectric phonograph pickup cartridge which generates a signal proportional to the sample's response.

The dynamic elastic modulus of a round bar sample is given by

$$E' = 1.606\left(\frac{L}{d}\right)^3\left(\frac{M}{d}\right)f^2 \tag{5}$$

where L is the length of the sample (cm), d is its diameter (cm), M is its mass (g), and f is its fundamental free-free resonant frequency (Hz). For a rectangular bar sample whose cross section has a horizontal dimension b (cm) and a vertical dimension h (cm),

$$E' = 0.94645\left(\frac{L}{h}\right)^3\left(\frac{M}{b}\right)f^2. \tag{6}$$

As a measure of internal friction,

$$Q^{-1} = \frac{\Delta f}{f} \tag{7}$$

is determined by the half-power bandwidth Δf at whose limits above and below the resonant frequency the response is 3 dB down from the maximum.

The test cell is cooled below 100°K with liquid nitrogen, then warmed up by an electrical heating element at a rate of about 1°K per minute. The resonant frequency and Q^{-1} are measured at 5°K intervals. In the present investigation, all tests were stopped at 345°K to avoid subjecting the samples to extended heat treatment at temperatures above their oven cure temperature. (Kreahling and Kline[16] found that a diglycidyl ether of bisphenol A cured with mPDA at 70°C had its properties changed by subsequent heat treatment at higher temperatures.)

Measurements of the dynamic elastic modulus over the temperature range from 85° to 345°K gave data points which lined up in curve families such as those shown in Figure 5 for samples filled with glass microspheres. All

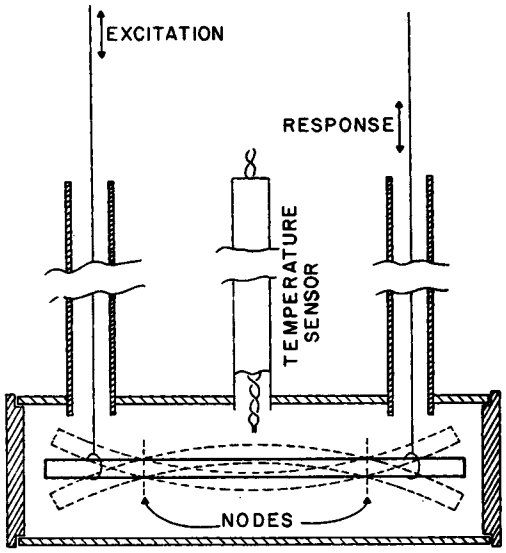

Fig. 4. Bar-shaped sample suspended in flexural resonance test cell.

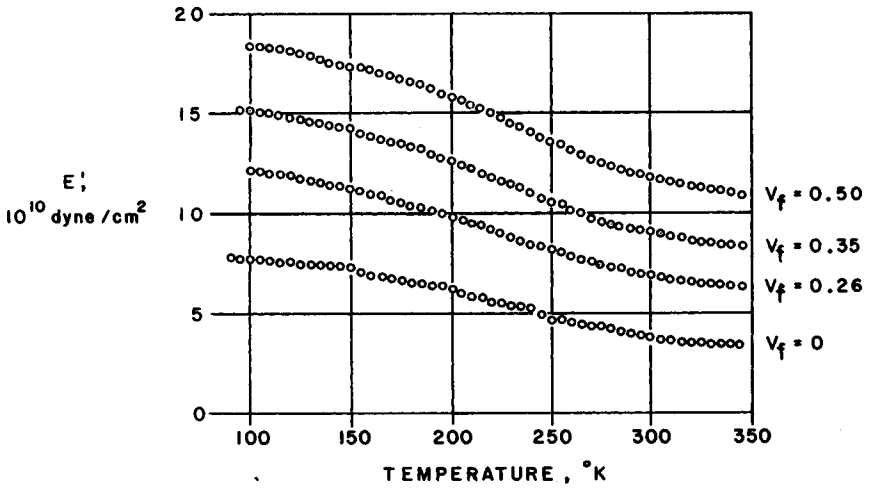

Fig. 5. Dynamic elastic moduli of glass microsphere–epoxy composites.

curves are of the same general form as that for the unfilled epoxy–mPDA matrix, the curve for $v_f = 0$. All fillers result in a composite modulus greater than the modulus of the unfilled polymer. For a given v_f, the use of fibrous fillers results in a greater increase in modulus and less temperature dependence than the use of particulate fillers.

The damping of glass-filled composites is shown in Figure 6. It is evident that fibrous fillers lower the damping more than particulate fillers, and there may be a tendency for all fillers to shift the 250°K peak to slightly higher temperatures. All the other fillers showed similar behavior.

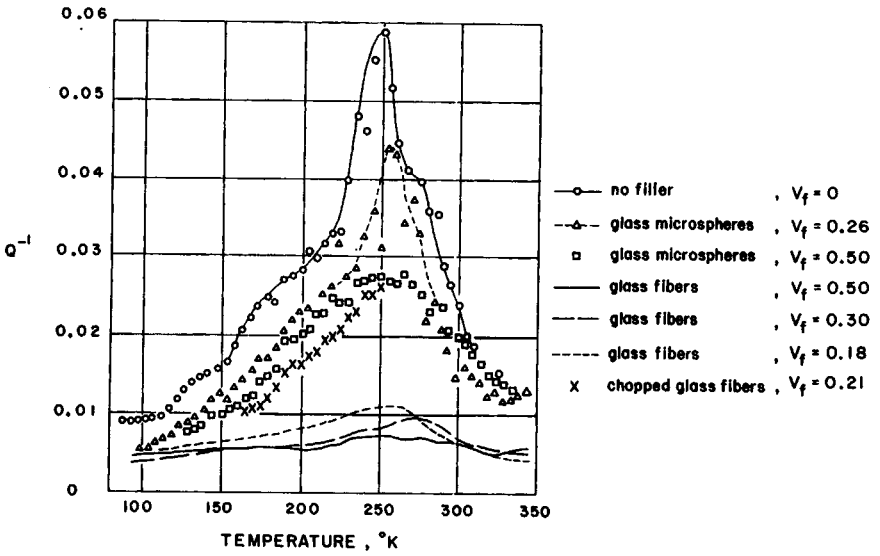

Fig. 6. Damping of particulate and fibrous glass–epoxy composites.

DISCUSSION

The Epoxy Matrix

The unfilled epoxy–mPDA system's behavior, shown by the data for $v_f = 0$ in Figures 5 and 6, is similar to that reported by Kreahling and Kline[16] for a monodispersed diglycidyl ether of bisphenol A (molecular weight 340) cured with a stoichiometric concentration of mPDA, with the same heat treatment as the present samples. The dynamic modulus of the present system is close to that of Kreahling and Kline at the lower end of the temperature range. In the higher range, it is about 5% below their modulus. The difference may result from the higher molecular weight constituents of the Epon 828 resin, which have greater chain lengths between epoxide endgroups than the monodispersed resin of Kreahling and Kline, leading to a lower crosslink density than that of their system.

The frequency of maximum response in the flexural resonance test is definite enough to make the dynamic modulus a continuous function of the temperature through the full temperature range, but in the vicinity of the 250°K relaxation the resonance peaks (curves of sample response as a function of driving frequency) are often asymmetric. Measurements of Q^{-1} are not of high precision. Nevertheless, even though the data points in Figure 6 scatter, it is quite evident that the matrix has a prominent damping peak in the vicinity of 250°K.

This peak appears quite similar to that observed by Kline[7] and by Kline and Sauer[8] in this temperature range for samples with the same resin and curing agent in very nearly the same ratio, with similar heat treatment. It is higher than a peak observed by Kreahling and Kline[16] in the same

temperature range. Kreahling and Kline also observed a peak at about 150°K, which appears in the present system as no more than a slight shoulder on the side of the 250°K peak. The greater height of the 250°K peak in the present system is to be expected with the greater modulus change, from about the same value as that reported by Kreahling and Kline at low temperatures to a value less than their higher-temperature value.

A number of investigators[9-13] attribute the 250°K damping peak to crankshaft motion of the ether linkages in the resin molecule. Kline[7] and Hirai and Kline[18] found the height of this peak increased as the portion of reacted epoxides increased. It appears that crankshaft motion of the ether linkages cannot take place until the epoxide triangles are opened and the loose ends of the resin molecule chains are attached to the polymer network. The 250°K damping peak and its associated decrease in the dynamic elastic modulus appear to be the result of a transformation from an almost completely immobilized system to a crosslinked network of stiff chain segments interspersed with loose crankshaft linkages.

Fibrous Composites

Figure 7 shows the dynamic modulus of glass fiber–epoxy composite samples at 300°K as a function of v_f. For the samples with long parallel glass fibers, v_f was determined by eq. (1). The rule-of-mixtures line is drawn from the 300°K value of the matrix dynamic modulus, 3.82×10^{10} dynes/cm^2, at $v_f = 0$ toward Owens-Corning's value[32] of the modulus of E

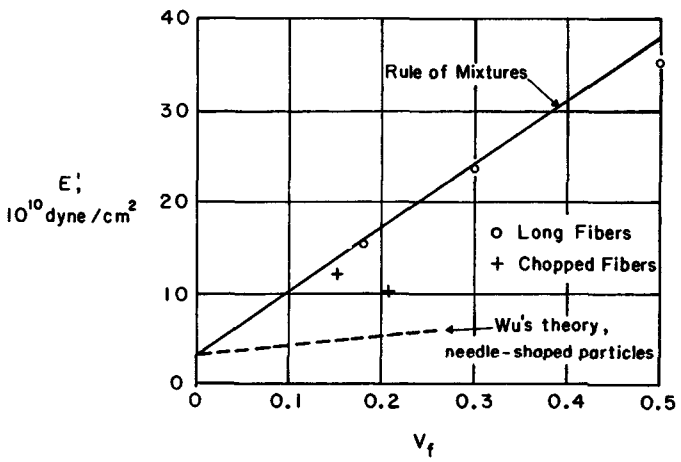

Fig. 7. Dynamic elastic moduli of glass fiber-epoxy composites as function of volume fraction of fibers, v_f, at 300°K. Rule-of-mixtures line based on matrix dynamic modulus of 3.82×10^{10}, dynes/cm^2 at 300°K and Owens-Corning's modulus of 72.5×10^{10}, dynes/cm^2. Dashed curve based on Wu's theory of particulate composite with needle-shaped filler particles with glass modulus is reference for randomly oriented chopped fibers; chopped fiber data points above Wu curve indicate some degree of parallel orientation.

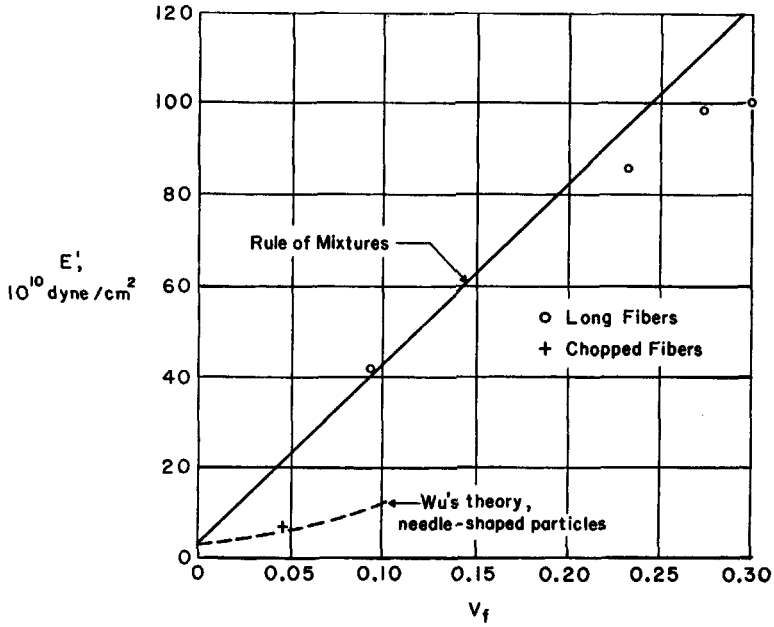

Fig. 8. Dynamic elastic moduli of graphite fiber–epoxy composites as function of volume fraction of fibers, v_f, at 300°K. Rule-of-mixtures line based on matrix dynamic modulus of 3.82×10^{10} dynes/cm^2 at 300°K and Great Lakes' modulus of 400×10^{10} dynes/cm. Fiber breakage at higher values of v_f causes composite modulus to fall below rule-of-mixtures line. Dashed curve based on Wu's theory of particulate composite with needle-shaped filler particles with modulus of carbon fibers. Data point of chopped fiber-filled sample near Wu curve indicates random orientation of chopped fibers.

glass fibers, 72.5×10^{10} dynes/cm^2, at $v_f = 1.0$. (Since the highest value of v_f in any sample is 0.5, only half the rule-of-mixtures line is included.) Data points for parallel fiber composite samples lie near this line in the lower range of v_f, but at the highest value of v_f the data point falls below the line. This is probably due to breakage and misalignment of tightly packed fibers during compression of the rectangular bar mold assembly (Fig. 1), a practical difficulty limiting the range of v_f over which the potential of parallel fiber composites fabricated by this technique can be realized. (It should be noted that the standard for comparison is not $v_f = 1.0$ but $v_f = 0.9069$, the value for close hexagonal packing of parallel cylinders.)

The rule-of-mixtures relationship is based on a simple equal strain theory. With equal axial strain in the low-modulus matrix and high-modulus fibers, the stress in the fibers is much greater than that in the matrix between them. With most of the strain energy in the low-damping fibers, the damping of a fibrous composite sample is much lower than that of an unfilled matrix sample, as seen in Figure 6.

Similar results were observed in graphite fiber–epoxy composite samples, Figure 8. The modulus of Great Lakes Fortafil 6T fibers[33] 400×10^{10}

dynes/cm^2, is much greater than the matrix modulus. The graphite fiber tows are looser than the glass fiber rovings and the graphite fibers are not of round cross section, so close packing is more difficult than it is in the case of the round Owens-Corning E glass fibers. As a result, stresses which build up during the mold compression operation are not as evenly distributed as they are in the glass fiber bundles. Stress concentrations begin to break some of the graphite fibers at lower values of v_f than in the molding of glass fiber composite samples. This appears to be the reason the data points for long fiber composite samples fall below the rule-of-mixtures line in Figure 8 at lower values of v_f than for the glass fiber composites, Figure 7. For samples in which fibers have broken and slipped out of the mold during fabrication, eq. (1) in inadequate, so eq. (3) was used for computation of v_f for these samples. (Resin-impregnated fiber bundles have relatively few voids, and those present can usually be detected and filled before the fibers are laid in the mold.)

In a bar-type composite sample with long parallel high-modulus fibers in a low-modulus matrix, the longitudinal Young's modulus is much greater than the longitudinal shear modulus, so the end-shear effect neglected in the derivation of the Bernoulli-Euler equation becomes significant. Flexural resonance must be interpreted on the basis of Timoshenko's analysis[34,35] rather than the Bernoulli-Euler equation. Dolph[36] has compiled Timoshenko corrections of the Bernoulli-Euler resonant frequency for free-free modes.

To use Dolph's curves as nomograms, preliminary estimates of the longitudinal Young's modulus and shear modulus are required. The dynamic modulus computed from the Bernoulli-Euler resonant frequency by eq. (6) can be used as a first-order estimate of the longitudinal Young's modulus. The longitudinal shear modulus G_L can be computed by Tsai's formula[37]

$$G_L = G_m \frac{2G_f - (G_f - G_m)(1 - v_f)}{2G_m - (G_f - G_m)(1 - v_f)}. \tag{8}$$

The matrix shear modulus G_m and fiber shear modulus G_f are each computed from the Young's moduli E_m and E_f by

$$G = \frac{E}{2(1 + \nu)} \tag{9}$$

where ν is Poisson's ratio. For the matrix, the Poisson ratio $\nu_m = 0.334$ found by Novak and Bert[38] is used. For the E glass fibers,[32] $\nu_f = 0.22$, and for the graphite fibers,[33] $\nu_f = 0.2$. For the glass fiber–epoxy composite samples, Dolph's Timoshenko correction increased the Bernoulli-Euler dynamic modulus by no more than 3%. However, the extreme anisotropy of the graphite fiber–epoxy composite samples made the corrected dynamic elastic modulus as much as 8% greater than that computed by eq. (6).

Particulate Composites

Parallel fiber composites have high strength and high moduli in the direction of fiber alignment, but their anisotropy may lead to the failure of a structural part by shear at an unexpected location. Furthermore, the alignment of fibers along a designer's predicted trajectories of maximum tensile stress may present formidable practical difficulties in the fabrication of a structural part. On the other hand, many types of particulate composites are macroscopically homogeneous and isotropic and can be molded by simple casting techniques. It is of interest to analyze the properties of the same epoxy matrix with some typical particulate fillers.

Damping

Nielsen[39] suggests that damping in a particulate composite should follow a rule-of-mixtures law like that of the modulus of a parallel fiber composite. Then, with damping Q_m^{-1} in the matrix and Q_f^{-1} in the filler, the damping Q_c^{-1} of the composite should conform to

$$\frac{Q_c^{-1}}{Q_m^{-1}} = 1 - v_f\left[1 - \frac{Q_f^{-1}}{Q_m^{-1}}\right]. \tag{10}$$

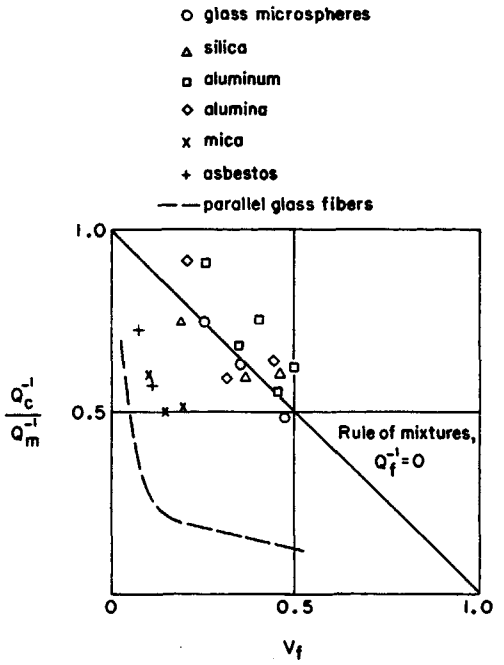

Fig. 9. Relative damping of composites with low-damping fillers at 250°K damping peak. Parallel glass fibers give large reduction of damping. Particulate fillers with quasi-spherical filler particles follow rule of mixtures; scatter of data points above and below line is indicative of lack of precision of damping measurements, and greater scatter above line indicates interface slippage. Asbestos and mica data points below line indicate behavior intermediate between particulate and fibrous composites.

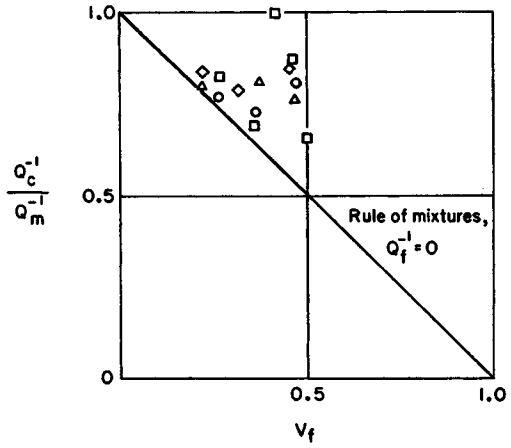

Fig. 10. Relative damping of particulate composites at 300°K. Data points above rule-of-mixtures line indicate interface slippage.

With a low-damping filler, the behavior should be approximately according to eq. (10) with $Q_f^{-1} = 0$, represented by the line in Figure 9. Data points for glass microspheres, silica, alumina, and aluminum fillers scatter along the line. The distance of the points below the line is probably no more than an indication of the low precision of the Q^{-1} measurements, since, according to eq. (10), even a filler with zero damping should not give points below the line. The points scatter farther above the line than below it. This could indicate that the fillers have small but finite damping. It could also indicate that there is more damping than that due to the matrix and filler particles; there may be some internal friction from slippage at the interface between them.

Asbestos and mica fillers lower the damping more than the spherical and quasi-spherical filler particles. This probably indicates that these materials have damping low compared to that of the matrix and that, because of their large length/thickness ratio, their damping behavior is intermediate between that of quasi-spherical particles and parallel fibers. They take up more of the strain energy than quasi-spherical filler particles but less than long parallel fibers. Their data points in Figure 9 lie between the rule-of-mixtures line and the Q_c^{-1}/Q_m^{-1} curve for the parallel glass fiber samples.

Figure 10 compares the rule-of-mixtures line for low-damping particulate fillers with the composite/matrix damping ratios resulting from the spherical and quasi-spherical filler particles at 300°K. The data points all lie above the line, indicating higher damping than that due to the matrix and filler. Internal friction from slippage at the filler–matrix interface is probably higher than that in the vicinity of the 250°K damping peak, Figure 9. Apparently the matrix, with a greater thermal expansion coefficient than the filler particles, shrinks tightly around them at lower

temperatures and restrains the interface slippage. Also, the matrix is more glass-like at lower temperatures. In the higher temperature range, the matrix expands, loosens the filler particles, and probably permits more interface slippage.

Nielsen[1] has noted a tendency for glass transition damping peaks to broaden with increasing filler content. The 250°K peak is not associated with the epoxy–mPDA system's primary glass transition, but with a limited secondary relaxation. It does appear to broaden as v_f increases, but Figure 6 shows the broadening biased slightly toward the high-temperature side of the peak.

This may be a thermal strain effect. With greater thermal expansion than that of the filler particles, the matrix probably shrinks around them at temperatures below the glass transition temperature or, in the present system, below the oven cure temperature. Below 300°K, the filler particles are probably subjected to compression as a result of this, and there are probably regions where the matrix is under tension. By analogy to the tension–frequency relationship in a vibrating string, polymer chain segments under tension may require greater thermal energy to initiate their motions. In regions of the matrix near the surfaces of filler particles, there may be steric hindrance to chain segment motions. An explanation suggested by several investigators[19,40,41,42] is the adsorption of a layer of immobilized polymer chains on the surface of the filler particles. It is postulated that polymer chains within these layers require greater thermal energy to set crankshaft linkages in motion.

Dynamic Elastic Modulus of Composites with Spherical Filler Particles

The elastic modulus of a particulate composite is a more complex function of v_f than the simple rule of mixtures for a parallel fiber composite. A number of theories have been developed to explain the stress–strain behavior of particulate composites, but since the size, shape, and arrangement of a large number of particles are difficult to describe, micromechanical models can only be based on averages and approximations.

By a presumed analogy between stress–strain relationships in elastic solids and stress–strain rate relationships in viscous liquids, viscosity theories have been converted into modulus theories. The formula of Mooney[3] gives a reasonable estimate of the behavior of a particulate-filled elastomer, but its modulus estimate is too high for a composite with a rigid polymer matrix. This is partly due to the fact that a theory for solid spheres suspended in a liquid deals with particles whose viscosity is effectively infinite relative to that of the liquid between them, while the filler modulus–matrix modulus ratio in a solid composite is finite. Also, the Poisson ratio of a rigid polymer is closer to $1/3$ than to the value $1/2$ usually associated with an elastomer.

In a direct approach to the stress–strain behavior of a solid particulate composite, Hashin and Shtrikman[2] have established rigorous upper and lower bounds to the modulus of a composite by strain energy analyses.

However, the gap between them is too wide to permit useful predictions of experimental results.

Others have examined the behavior of individual filler particles and the matrix region surrounding them, then derived models to approximate the behavior of large numbers of such inclusions. Goodier[43] found an exact solution to the problem of a single spherical inclusion in a block of matrix material subjected to a uniform stress with no slippage at the interface. He points out that, by St. Venant's principle, the inclusion's perturbation of the strain field is effectively smoothed out within a relatively small distance. Thus, if particles do not approach each other too closely, a particulate composite can be treated as an array of such sphere-containing blocks, with its apparent modulus given by Goodier's solution to the problem of a single spherical inclusion with properties different from those of the surrounding matrix. This of course is effective only over the lower range of v_f.

Kerner[4] has applied Goodier's method to seek an effective value of the modulus for higher values of v_f. He takes as his model a spherical filler particle surrounded by a shell of matrix material, which is in turn surrounded by an infinite medium assumed to have the macroscopic properties of the composite. He also assumed no slippage at the concentric spherical interfaces. The result is one of the less complex expressions relating the properties of the composite to those of the matrix and filler. For a matrix of modulus E_m and Poisson ratio ν_m filled with spherical particles of modulus E_f with the same Poisson ratio, Hirai and Kline[28] express the Lewis-Nielsen form of Kerner's equation[24] as

$$\frac{E_c}{E_m} = \frac{1 + ABv_f}{1 - Bv_f} \tag{11}$$

where

$$A = \frac{7 - 5\nu_m}{8 - 10\nu_m}$$

$$B = \frac{(E_f/E_m) - 1}{(E_f/E_m) - A}.$$

Assuming a composite's dynamic modulus E_c' (measured by the flexural resonance technique[31]) conforms to the same micromechanical models as its static modulus E_c, Figure 11 compares Kerner's formula with data from samples filled with glass microspheres. The modulus of the glass in the microspheres is not known. However, available data[44] indicate that all silica-based glasses have about the same modulus. Taking the E glass modulus (about 20 times the dynamic modulus of the epoxy–mPDA matrix at room temperature) as an approximation to the modulus of the glass in the microspheres, E_f/E_m was assigned the value 20. For ν_m, the tensile Poisson ratio 0.334 found by Novak and Bert[38] was used. Although their data are for a different epoxy system, this appears to be the most probable value for the Poisson ratio of the present system as well. (Their

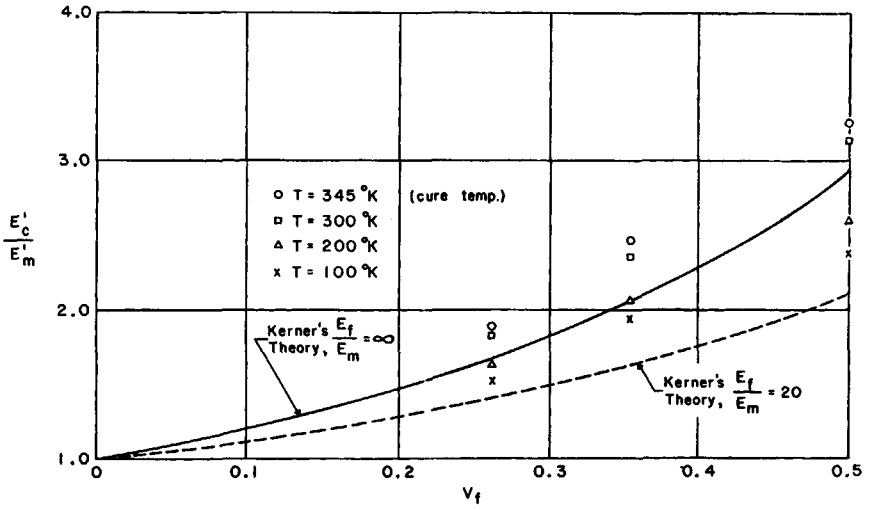

Fig. 11. Ratios of composite dynamic modulus E_c' to matrix dynamic modulus E_m' for glass microsphere-epoxy composites compared to Kerner's theory for a composite with spherical filler particles. Lower curve based on Kerner's formula with filler modulus 20 times matrix modulus; upper curve based on infinite filler modulus.

tensile modulus, 0.547×10^6 psi, is quite close to the dynamic modulus 3.82×10^{10} dynes/cm^2 of the present system at 300°K.)

Regardless of the temperature, all the data points lie above the Kerner curve for $E_f/E_m = 20$. The curve for $E_f/E_m = \infty$ is also included for reference; the higher-temperature data points lie above this curve as well. A similar increase in the composite/matrix modulus ratio with temperature was observed by Hirai and Kline[28] for the epoxy–DETA system filled with carbon and graphite particles, and by Lewis and Nielsen[24] for epoxy–triethylenetetramine filled with glass microspheres. Nielsen and Lewis[23] suggest that it is a thermal strain effect, and later work by Nielsen and Lee[45] lends further support to their theory. They assume the matrix, with a greater thermal expansion coefficient than that of the filler particles, shrinks around them as the system cools below the curing temperature, putting the matrix in tension. This biases it to a higher point on its non-linear stress–strain curve, where the slope (which determines the small-strain dynamic modulus) is lower than the zero-strain modulus. If the actual matrix modulus in the composite is lower than that of the unfilled matrix sample used as the $v_f = 0$ reference, the dynamic modulus ratio E_c'/E_m' will be too low when the unfilled sample's dynamic modulus is taken for E_m'. Then the unfilled sample's modulus can be used as E_m' in this ratio only when there is no thermal strain. For samples cured at 70°C (343°K), there should be very little thermal strain at 345°K, the upper limit of the temperature range over which the dynamic modulus is measured. Therefore, all further comparisons to be made here between

the dynamic moduli of samples and theoretical models will be based on data taken at this temperature.

Since the modulus ratios predicted by Kerner's formula are considerably lower than the experimental values at 345°K, it is of interest to consider another theory. Lewis and Nielsen[24] also found Kerner's predictions too low and pointed out that Kerner's formula is equivalent to the lower bound of Hashin and Shtrikman[2]. They modified eq. (11) by a correction factor in the second term of the denominator, making it a more complex function of v_f. However, rather than adjusting Kerner's formula, it is of more interest to compare experimental data with the more recent particulate composite theory of Wu.[5]

In a development similar to Kerner's use of Goodier's spherical inclusion model, Wu bases his theory on Eshelby's treatment of the strain field resulting from an ellipsoidal inclusion in a homogeneous isotropic matrix. Eshelby[46] shows that if there is no slippage at the interface, an ellipsoidal inclusion with elastic constants different from those of the matrix has uniform stress within it when the matrix is subjected to a uniform stress at a large distance from the inclusion. In the determination of an effective composite modulus, the stress at intermediate points in the matrix need not be known. Wu[5] generalizes the result for a large number of closely spaced ellipsoidal inclusions, averaging over all orientations to arrive at an expression for the modulus of a composite filled with randomly oriented ellipsoidal filler particles.

Of course, few if any actual fillers have ellipsoidal particles. However, three special cases are of direct practical interest. The simplest form of ellipsoid is the sphere. Spherical glass filler particles are available, and Nielsen[1] suggests that theories for spherical filler particles should also apply to those that are approximately spherical. The limit toward which oblate spheroids tend is the thin flat disc; some filler particles are thin flat flakes which may approximate the behavior of this model. The other extreme form of ellipsoid is the prolate spheroid extended to a thin rod or needle; short fiber fillers may conform to this model. Thus, Wu's theory predicts the composite moduli resulting from three common filler particle shapes.

Wu's formulas are cumbersome and quite tedious to apply. However, they become manageable when numerical values of the elastic moduli and Poisson ratios of the matrix and filler are inserted. With $E_f/E_m = 20$, the value $\nu_m = 0.334$ of Novak and Bert,[38] and the E glass value[32] $\nu_f = 0.22$, Wu's formula[5] for the modulus of a composite with spherical filler particles reduces to a quadratic equation from which the solid curve in Figure 12 was plotted. (For comparison, the Kerner curve for $E_f/E_m = \infty$ from Fig. 11 is included.)

This equation contains a residual unspecified quantity ν_c, the Poisson ratio of the composite, which is also a function of v_f. This Poisson ratio does not exert a strong influence on the computed value of E_c and was neglected by Wu[5] in the illustrative examples at the conclusion of his paper, for which he assumed $\nu_c = \nu_m = \nu_f = 0.2$. However, for $\nu_f \neq \nu_m$,

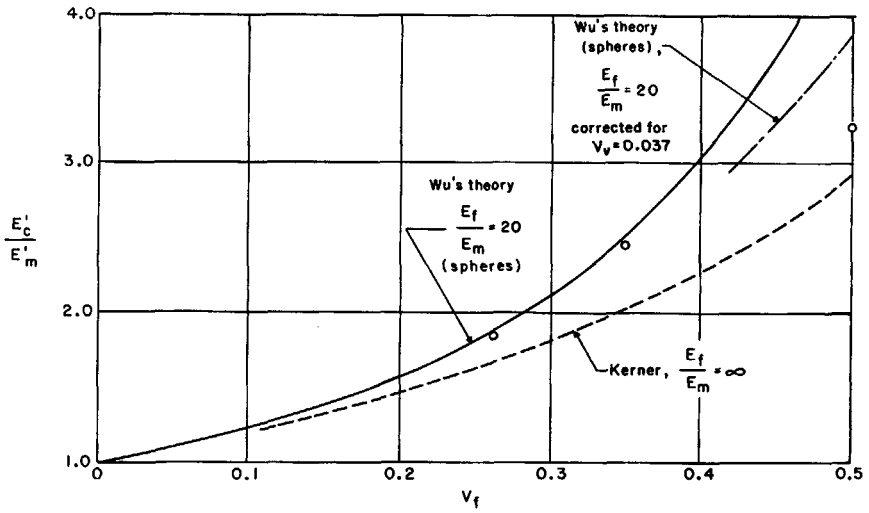

Fig. 12. Ratios of composite dynamic modulus E_c' to matrix dynamic modulus E_m' for glass microsphere–epoxy composites compared to theories of Kerner and Wu, at 345°K.

it is reasonable to expect ν_c to approach ν_m at low v_f and ν_f at high v_f. Taking $\nu_c = \nu_m$ in Wu's formula makes $E_c/E_m = 1$ at $v_f = 0$, but the curve then intersects $v_f = 1$ at a point where $E_c/E_m > E_f/E_m$. On the other hand, the curve generated by taking $\nu_c = \nu_f$ in Wu's formula falls to $E_c/E_m = 1$ at a finite value of v_f. To improve the precision of the Wu curve in Figure 12, a first-order interpolation was made between these two curves. At each value of E_c/E_m, the v_f coordinate was taken as that of the curve for $\nu_c = \nu_m$ plus a fraction v_f of the v_f difference between it and the curve for $\nu_c = \nu_f$. This may not be in strict conformity with Wu's theory, but the difference between the two curves is not large; any errors introduced by this ν_c adjustment should be rather small.

Of course, there is an obvious question of the validity of Wu's theory at high v_f. Wu's formulas express a continuous functional relationship between E_c/E_m and v_f over the full range of v_f from 0 to 1.0. However, with spheres of uniform diameter in close regular packing,[47] the maximum possible value of v_f is 0.74. In the present work, this value was not approached; it is of primary interest to compare the data with the Wu curve in Figure 12 in the range $0 < v_f < 0.5$.

The data points in Figure 12 lie near the Wu curve at the lower values of v_f, but the point for the highest value of v_f falls well below it. It is postulated that this is due to voids; air entrained by the filler particles could not be completely evacuated from filled resin mixtures with v_f greater than 0.35 to 0.40.

In their work on epoxy–DETA filled with carbon and graphite particles, Hirai and Kline[28] derived a void correction factor based on Wu's formula for spherical filler particles[5] by assuming a composite with voids to be a

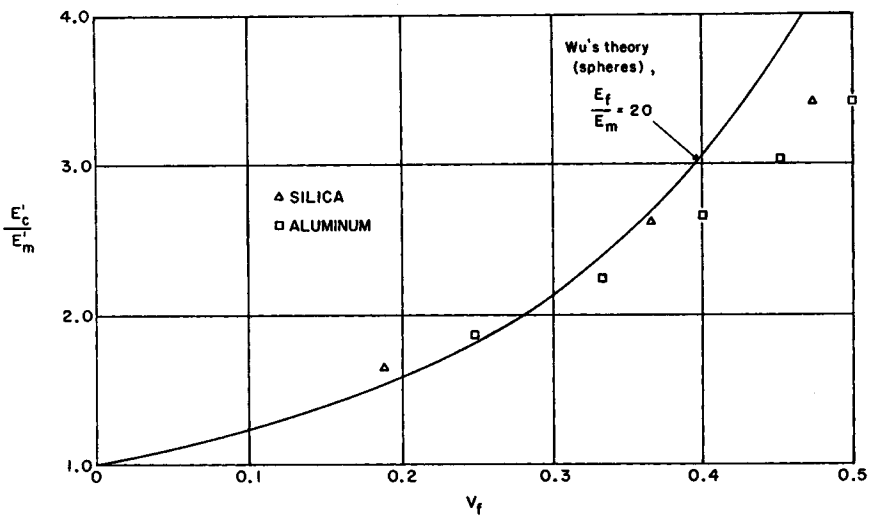

Fig. 13. Ratios of composite dynamic modulus E_c' to matrix dynamic modulus E_m' for aluminum–epoxy and silica–epoxy composites compared to Wu's theory of a particulate composite filled with spherical particles, at 345°K.

homogeneous material containing spherical particles of zero modulus. They assumed a composite Poisson ratio $\nu_c = 0.2$, which leads to

$$\frac{E_{cv}}{E_c} = 1 - 2v_v \tag{12}$$

where E_{cv} is the modulus of a composite with a volume fraction of voids v_v determined by eq. (4). (This gives a conservatively pessimistic estimate. With a higher value of ν_c, the coefficient of the second term is somewhat less than 2.)

The sample with the highest value of v_f in Figure 12 had a void content $v_v = 0.037$ and the void-correction factor computed by eq. (12) is 0.93. Inserting 0.93 E_c in place of E_c in Wu's formula generates the curve segment (shown by — - — -) below the solid curve in the upper right-hand corner of Figure 12. The data point lies below this void-corrected Wu curve, so it appears that the sample may contain defects more significant than simple bubbles in a homogeneous filler–matrix mixture. There are probably regions of agglomerated filler particles which have not been dispersed into the matrix.

Aluminum has about the same modulus as glass, and the modulus of silica is also near this value.[44] Aluminum and silica particles are quasi-spherical in that they are neither flakes nor fibers, so it is of interest to compare these fillers with Wu's theory for spherical filler particles. Figure 13 reproduces the Wu curve of Figure 12 and presents data points for samples filled with silica and atomized aluminum. The silica-filled composite data points lie near the curve at low v_f and fall below it at high v_f in a manner similar to those in Figure 12. This again probably indicates

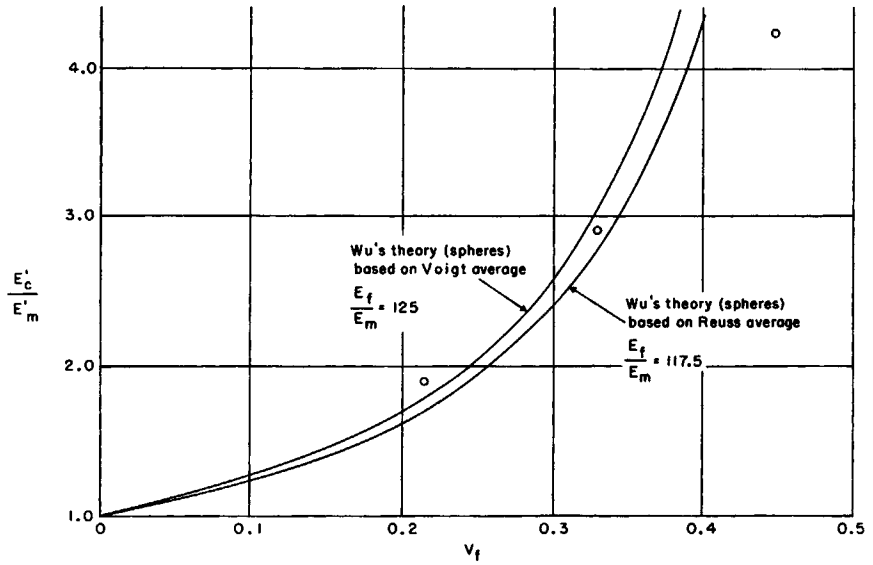

Fig. 14. Ratios of composite dynamic modulus E_c' to matrix dynamic modulus E_m' for alumina-epoxy composites at 345°K compared to Wu's theory of a particulate composite filled with spherical particles. Upper curve based on filler modulus equal to Voigt aggregate average for Al_2O_3 crystal; lower curve based on Reuss aggregate average.

defects in the composite sample with the highest filler concentration. This sample has a fairly low value of v_v, insufficient to explain the difference on the basis of the void correction factor calculated by eq. (12). Therefore, it appears that the silica particles, like the glass microspheres, have a tendency to agglomerate at values of v_f above 0.40. The data points for aluminum-filled samples also fall below the curve at the higher values of v_f, indicating that the aluminum filler particles also may have a tendency to agglomerate.

The alumina filler particles are also quasi-spherical, but require a new Wu curve for comparison, since E_f is considerably higher for alumina than for glass, silica, and aluminum. Furthermore, the alumina particles are anisotropic crystallites, so E_f must be an average value intermediate between the maximum and minimum moduli of the Al_2O_3 crystal.

To compute coordinates of points to plot a Wu curve for comparison with the data from alumina-filled samples, E_f and ν_f in Wu's formula for spherical filler particles[5] were taken from a compilation by Simmons and Wang[48] of the aggregate average values for randomly oriented crystalline particles. Their Voigt aggregate average values for alumina (based on the assumption of equal strains along the principal axes of randomly oriented crystallites) are $\nu_f = 0.233$ and $E_f = 4.01 \times 10^{12}$ dynes/cm^2, which is about 125 times the dynamic modulus of the matrix at 345°K. The Reuss aggregate average values (based on equal stress) are $\nu_f = 0.240$ and $E_f = 3.90 \times 10^{12}$ dynes/cm^2, for which $E_f/E_m = 117.5$.

Wu curves based on both the Voigt and Reuss values are presented in Figure 14, together with data points for samples filled with powdered alumina. The lower data point lies above both curves. Since the alumina particles are not perfect spheres, they should result in slightly higher values than Wu's sphere theory, which predicts that spheres are the filler particle shape which gives the least increase in modulus for a given value of v_f. For the highest value of v_f, the data point lies below both curves; again, the agglomeration of filler particles is considered to be the dominant cause.

Dynamic Elastic Modulus of a Composite with Disc-Shaped Filler Particles

Wu's theory predicts that filler particles in the form of thin discs should give the maximum increase in modulus for a given value of v_f. Mica filler particles are not round discs, but they are thin, flat flakes which might be expected to approximate the behavior of disc-shaped particles. The solid curves in Figure 15 were prepared from Wu's formula for disc-shaped filler particles[5] by the same general procedure as that for the curves in Figure 14. For the muscovite mica crystal, Simmons and Wang[48] list Voigt aggregate average values $\nu_f = 0.227$ and $E_f = 1.008 \times 10^{12}$ dynes/

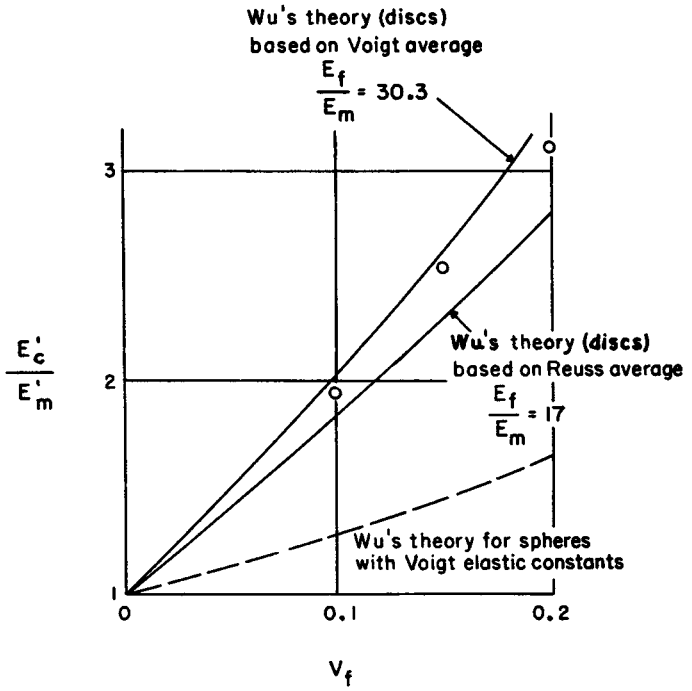

Fig. 15. Ratios of composite dynamic modulus E_c' to matrix dynamic modulus E_m' for mica–epoxy composites at 345°K compared to Wu's theory of a particulate composite with disc-shaped filler particles. Upper curve based on filler modulus equal to Voigt aggregate average for muscovite crystal; lower curve based on Reuss aggregate average. Curve based on Wu's theory for spnerical filler particles with Voigt aggregate average modulus shown at bottom for comparison.

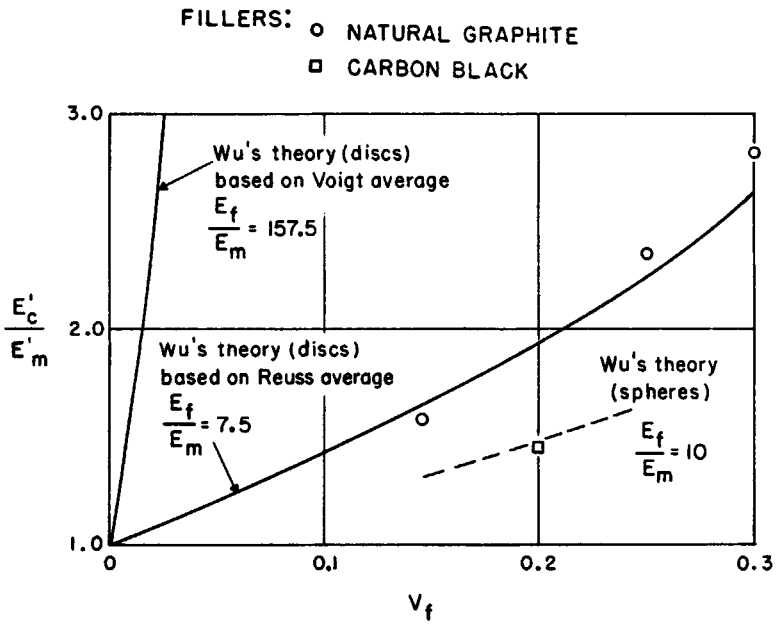

Fig. 16. Ratio of composite dynamic modulus E_c' to matrix dynamic modulus E_m' for graphite–epoxy composites at 345°K compared to Wu's theory of a particulate composite with disc-shaped filler particles. Upper curve based on filler modulus equal to Voigt aggregate average for graphite crystal; lower curve based on Reuss aggregate average. Segment of Wu curve for spherical filler particles with ten times matrix modulus included for comparison with data point from carbon black–epoxy composite sample.

cm^2 = 30.3 E_m. The Reuss-average values are ν_f = 0.279 and E_f = 0.568 × 10^{12} dynes/cm^2 = 17 E_m. The data points in Figure 15 lie between the Wu curves based on the Voigt and Reuss values, giving considerable support to Wu's theory for disc-shaped filler particles. Comparison of Figures 14 and 15 shows that quasi-spherical alumina particles result in a considerably lower modulus ratio at low v_f, even though their modulus is about four times that of the mica flakes. It is evident, both in the theoretical Wu curves and in the experimental data points, that the shape of the filler particles is more decisive than their modulus. For comparison, a Wu curve for spherical filler particles with the Voigt parameters of mica is included in Figure 15.

Graphite flakes might also be expected to conform to Wu's theory for disc-shaped filler particles. However, the situation is complicated by the extreme anisotropy of the graphite crystal. The curves in Figure 16 are based on Voigt and Reuss aggregate values of ν_f and E_f computed by Hearmon's formulas[49] for average values of the elastic constants of anisotropic crystallites. Values of the graphite crystal elastic constant[2] recently presented by Kelly[50] were used in these calculations, leading to Voigt-average values ν_f = 0.197 and E_f = 524 × 10^{10} dynes/cm^2 = 157.5 E_m and Reuss-average values ν_f = 0.390 and E_f = 25 × 10^{10} dynes/cm^2 =

7.5 E_m. The Wu curves based on these Voigt and Reuss values in Figure 16 diverge widely.

The data points for the samples filled with SP-1 natural graphite flakes lie near the Wu curve based on the Reuss values. This may be associated with the anisotropy of the graphite crystals and the large diameter/thickness ratio of the particles. Most of the filler–matrix contact is on the faces orthogonal to the *c*-axis of the graphite crystallites, with only a small portion of the total interface area at the edges. This is favorable for the transmission, between the matrix and the filler particles, of both basal-plane shearing stresses and normal stresses in the *c*-axis direction. The filler particles have their highest compliances for these stresses, so they might be expected to deform in such a manner as to distribute the strains in an approximation of the Reuss equal-stress model. At least it is obvious that the Voigt equal-strain model is inappropriate for the highly anisotropic graphite filler particles.

The data point for the sample with the highest concentration of graphite flake filler in Figure 16 lies significantly above the Wu-Reuss curve. This may be due to partial orientation of the graphite flakes with their high-modulus axes parallel to the axis of the sample. Wu's theory assumes random orientation of the particles; but as v_f increases, anisotropy can be expected to occur at some stage.

A thin disc of diameter d and thickness t, free to assume any orientation, must be assigned a spherical volume $\pi d^3/6$, even though it actually occupies a volume $\pi d^2 t/4$. The ratio of its actual volume to its random orientation volume is then $^3/_2 t/d$. The maximum volume fraction possible for close-packed spheres[47] is 0.74, so the volume fraction below which disc-shaped filler particles might have freedom of orientation is

$$v_{fd} = 0.74\left(\frac{3}{2}\frac{t}{d}\right) = 11.1\,\frac{t}{d}. \tag{13}$$

Equation (13) is not to be assigned any great significance, since random orientation of a large number of discs may still be possible even though many of them intrude into the random orientation spheres of others. However, it is of interest to note that Taylor, Kline, and Walker[51] found the SP-1 natural graphite flakes to have an average diameter of about 30 μm and an average thickness of about 0.5 μm. With $t/d = 1/60$, eq. (13) indicates that some loss of randomness in the orientation of the graphite flakes may begin with v_f as low as 0.02. Still, it is possible for the overall orientation to remain random on a macroscopic scale if the orientations of small, parallel-stacked domains are distributed over all directions. This appears to be valid in Figure 16 up to a v_f value of about 0.25. (The distances of the points for $v_f = 0.15$ and 0.25 from the curve probably indicate no more than the experimental spread of the data.)

In contrast to graphite, carbon black is the least effective filler in the present series for increasing the modulus of a composite. Its particles are approximately spherical and behave in the epoxy matrix as a filler with a

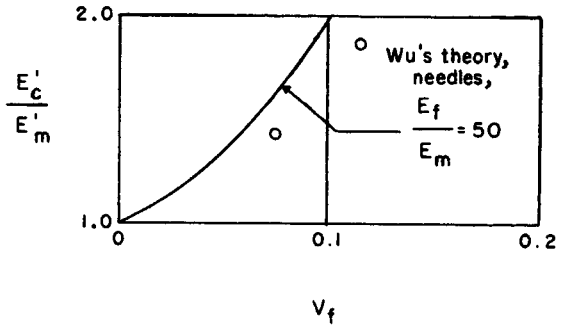

Fig. 17. Ratios of composite dynamic modulus E_c' to matrix dynamic modulus E_m' for asbestos–epoxy composites at 345°K compared to Wu's theory of a prticulate composite with needle-shaped filler particles. Filler modulus assumed equal to modulus of asbestos fibers, 170×10^{10} dynes/cm^2. Data points fall below curve; filler particles not all needle-shaped.

modulus about ten times that of the matrix, a result also noted by Hirai and Kline.[28] For reference, Figure 16 includes a segment of a Wu curve for spherical filler particles with $E_f/E_m = 10$ and a data point for a carbon black–epoxy composite sample. Payne, Whittaker, and Smith[41] have noted that carbon black filler particles are actually agglomerates of much smaller particles. They are broken up into smaller agglomerates by stirring into a polymer matrix, but these tend to remain together in long chains. Such entities might behave in a manner similar to chopped fibers or needle-shaped filler particles. This offers an explanation of the fact that carbon black could not be mixed into the matrix in much greater concentration than the asbestos and mica fillers.

Dynamic Elastic Modulus of a Composite with Needle-Shaped Filler Particles

The other extreme in the filler particle shapes considered by Wu[5] is needles, whiskers, or chopped fibers. The modulus of asbestos fibers has been given[52] as about 170×10^{10} dynes/cm^2, or 50 times that of the matrix at 345°K; this value of E_f was used in Wu's formula for the modulus of a composite with needle-shaped filler particles[5] to plot the curve in Figure 17. Data points lie below this curve. This is probably due in part to voids, but may also be due to the fact that the asbestos filler contains some quasi-spherical granules in addition to the fibrous particles and thus is not entirely a needle-type filler. It may also be due to an error in the value[52] assumed for the modulus of the asbestos filler.

Needle-shaped filler particles, of course, can become oriented parallel to each other so that they no longer conform to Wu's theory. By a derivation similar to that of eq. (13), it can be shown that a short fiber of length d and thickness t has an actual volume $\pi dt^2/4$, a random orientation volume $\pi d^3/6$, and a free orientation volume fraction

$$v_{fn} = 1.11\left(\frac{t}{d}\right)^2. \tag{14}$$

Again, no great significance is to be attached to numerical values computed by this formula, but it does show that needle-type filler particles tend to interfere with each other at a very low v_f. This offers some explanation of the difficulties encountered in achieving large values of v_f in samples filled with asbestos and chopped fibers.

Composites with short-fiber or needle-shaped filler particles can have properties intermediate between those of particulate and parallel fiber composites. If the needles or chopped fibers have lengths large compared to their diameters and are oriented parallel to each other, the composites have very nearly the same properties as long fiber composites in the direction parallel to the fibers. In a direction orthogonal to the fibers, their properties are similar to those of a particulate composite with quasi-spherical filler particles. With completely random orientation of chopped fibers, the composite should conform to Wu's theory for a particulate composite with needle-shaped filler particles. In practice, chopper fiber composites usually have their fibers partially oriented, conforming neither to Wu's theory nor to the parallel fiber model.

Wu's formula for needle-shaped filler particles[5] with the elastic constants of the glass and graphite fibers was used to plot the dashed curves in the lower left-hand area of Figure 7 and 8. Data points for chopped fiber-filled samples lie between these Wu curves and the rule-of-mixtures line for parallel fibers; the chopped fibers have neither complete randomness nor parallel orientation.

Practical Considerations

A summary of particulate–composite moduli at 300°K is compiled in Figure 18. Carbon black is the least effective filler for increasing the modulus, and asbestos and mica are the most effective. None of these can be mixed into the matrix in very high concentration.

Aluminum, silica, and glass microspheres all result in about the same modulus for a given value of v_f. Aluminum-filled composites are easily machinable, while glass and silica particles abrade cutting tools.

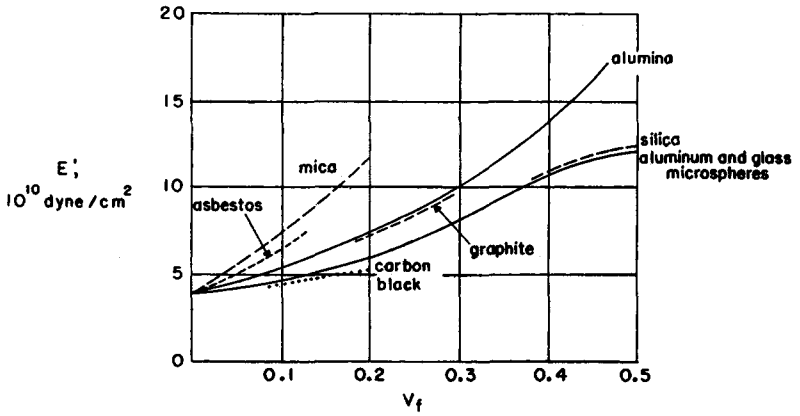

Fig. 18. Dynamic moduli of particulate epoxy composites at 300°K.

Graphite and alumina fillers result in very nearly the same modulus for a given value of v_f. The flat graphite flakes have a rather low aggregate-average modulus but result in a relatively high composite modulus because of their quasi-disc shape. Flake-type fillers are more effective than quasi-spherical particles in increasing the modulus of a composite, but they cannot be mixed into the matrix in sufficient concentration to occupy more than a minor portion of the total volume. This defeats one of the major purposes of particulate composites, the replacement of a relatively expensive matrix with cheap filler material. The alumina particles are quasi-spherical, but they equal or surpass the graphite flakes because of their high modulus. Because of their quasi-spherical shape, alumina filler particles can be mixed with the epoxy matrix up to higher values of v_f, leading to a continuation of the $E'(v_f)$ curve beyond the $v_f = 0.3$ limit for graphite. Of course, the hard alumina particles, like the glass and silica particles, abrade cutting tools; graphite-filled composites are more easily machined.

CONCLUSIONS

Dynamic elastic moduli have been determined at temperatures between 85° and 345°K for a number of composites with representative fillers in a stoichiometric Epon 828–mPDA matrix. The data appear to result in extensive experimental verification of Wu's theory of the elastic modulus of a particulate composite.[5]

Wu's theory appears to be valid for particulate composites reasonably free of defects such as voids and agglomerates of undispersed filler particles. It is based on a micromechanical theory-of-elasticity model and therefore constitutes an advance over previous theories which merely established upper and lower bounds or made use of a presumed viscosity-modulus analogy. Wu's formula for spherical filler particles is useful for fillers whose particles are only approximately spherical, i.e., those without obvious elongation or flattening. The formula for disc-shaped filler particles appears to be applicable to flat flake fillers whose particles are not necessarily round discs. For needle-shaped particles, the evidence is not as extensive; here, the situation is complicated by the practical difficulties involved in the mixing and pouring of resins filled with particles of this shape. Composites with disc- and needle-shaped filler particles may appear to deviate from Wu's theory because of the tendency of the particles to become oriented parallel to each other during the processes of sample preparation. Overall, the present work confirms Wu's theory for a variety of typical particulate fillers within the practical range of filler concentration.

Dynamic moduli of parallel fiber composites conform to the linear rule of mixtures at low fiber volume fractions. Deviations from linearity at higher volume fractions are probably due to breakage and misalignment of fibers resulting from the sample fabrication technique.

Damping in particulate composites with quasi-spherical filler particles appears to follow the rule of mixtures. In fibrous composites and in particulate composites with needle- and flake-type fillers, the fillers take up a greater portion of the strain energy and reduce the overall damping. Damping greater than that attributable to the matrix and filler probably indicates slippage at the interface between them.

In addition to confirming Wu's theory, this study demonstrates the validity of nondestructive free-free flexural resonance testing[31] as a research and engineering method. The elastic moduli and damping of a diverse variety of materials can be measured over a large temperature range. Theoretical models can be thoroughly tested, and the relative merits of various options in fillers, matrices, and additives can be compared. The effects of different fabrication techniques can be evaluated economically within a short time with relatively few small samples.

The authors are indebted to D. A. Whiting for infrared analysis and to P. R. Blankenhorn for assistance in dynamic mechanical testing. This work was supported in part by the U.S. Atomic Energy Commission.

References

1. L. E. Nielsen, *J. Comp. Mat.*, **1**, 100(1967).
2. Z. Hashin and S. Shtrikman, *J. Mech. Phys. Solids*, **10**, 335 (1962).
3. M. Mooney, *J. Colloid Sci.*, **6**, 162 (1951).
4. E. H. Kerner, *Proc. Phys. Soc.*, **69B**, 808 (1956).
5. T. T. Wu, *Int. J. Solids Structures*, **2**, 1 (1966).
6. D. H. Kaelble, *SPE J.*, **15**, 1071 (1959).
7. D. E. Kline, *J. Polym. Sci.*, **47**, 237 (1960).
8. D. E. Kline and J. A. Sauer, *SPE Trans.*, **2**, 1 (1962).
9. C. A. May and F. E. Weir, *SPE Trans.*, **2**, 207 (1962),
10. F. R. Dammont and T. K. Kwei, *J. Polym. Sci. A-2*, **5**, 761 (1967).
11. N. Hata and J. Kumanotani, *J. Appl. Polym. Sci.*, **15**, 237 (1971).
12. G. A. Pogany, *Polymer*, **11**, 66 (1970).
13. H. VanHoorn, *J. Appl. Polym. Sci.*, **12**, 871 (1968).
14. O. Delatycki, J. S. Shaw, and J. G. Williams, *J. Polym. Sci. A-2*, **7**, 753 (1969).
15. T. Murayama and J. P. Bell, *J. Polym. Sci. A-2*, **8**, 437 (1970).
16. R. P. Kreahling and D. E. Kline, *J. Appl. Polym. Sci.*, **13**, 2411 (1959).
17. T. Hirai and D. E. Kline, *J. Appl. Polym. Sci.*, **16**, 3145 (1972).
18. T. Hirai and D. E. Kline, *J. Appl. Polym. Sci.*, **17**, 31 (1973).
19. I. Galperin, *J. Appl. Polym. Sci.*, **11**, 1475 (1967).
20. A. B. Schultz and S. W. Tsai, *J. Comp. Mat.*, **2**, 368 (1968).
21. J. M. Lifshitz and A. Rotem, *J. Comp. Mat.*, **3**, 412 (1969).
22. J. H. Saxton and D. E. Kline, *J. Opt. Soc. Amer.*, **50**, 1103 (1960).
23. L. E. Nielsen and T. B. Lewis, *J. Polym. Sci.*, 1705 (1969).
24. T. B. Lewis and L. E. Nielsen, *J. Appl. Polym. Sci.*, **14**, 1449 (1970).
25. T. J. Dudek, *J. Comp. Mat.*, **4**, 232 (1970).
26. T. J. Dudek, *J. Polym. Sci. A-2*, **8**, 1575 (1970).
27. T. Hirai and D. E. Kline, *J. Comp. Mat.* in press.
28. T. Hirai and D. E. Kline, *J. Comp. Mat.* in press.
29. L. E. Nielsen, *Rev. Sci. Instr.*, **22**, 690 (1951).
30. F. Förster, *Zeitschr. Metallkunde*, **29**, 109 (1937).
31. D. E. Kline, *J. Polym. Sci.*, **22**, 449 (1956),

32. Owens-Corning Fiberglas Corp., Technical Bulletin, *Textile Fibers for Industry*, August 1971, p. 8.

33. Great Lakes Carbon Corp. Technical Sheet, *Fortafil 6T*, 1971.

34. S. P. Timoshenko, *Phil. Mag.*, **41**, 6, 744 (1921).

35. S. P. Timoshenko, *Phil Mag.*, **43**, 6, 125 (1922).

36. C. L. Dolph, *Quart. Appl. Math.*, **12**, 175 (1954).

37. S. W. Tsai, *Structural Behavior of Composite Materials*, National Aeronautics and Space Administration Report, NASA CR-71 July 1964.

38. R. C. Novak and C. W. Bert, *J. Comp. Mat.*, **2**, 506 (1968).

39. L. E. Nielsen, *Trans. Soc. Rheol.*, **13**, 141 (1969).

40. I. Galperin and T. K. Kwei, *J. Appl. Polym. Sci.*, **10**, 673 (1966).

41. A. R. Payne, R. E. Whittaker, and J. F. Smith, *J. Appl. Polym. Sci.*, **16**, 1191 (1972).

42. P. I. Zubov, L. A. Sukhareva, and V. A. Voronkov, *Polym. Mech.*, **3**, 507 (1967).

43. J. N. Goodier, *Trans. Amer. Soc. Mech. Eng.*, **55**, 39 (1933).

44. F. S. Galasso, *High Modulus Fibers and Composites*, Gordon and Breach, New York, 1969, p. 4.

45. L. E. Nielsen and B. L. Lee, *J. Comp. Mat.*, **6**, 136 (1972).

46. J. D. Eshelby, *Proc. Roy. Soc.* (London), **A241**, 376 (1967).

47. R. K. McGeary, *J. Amer. Cer. Soc.*, **44**, 513 (1961).

48. G. Simmons and H. Wang, *Handbook of Single-Crystal Elastic Constants and Calculated Aggregate Properties*, The M.I.T. Press, Cambridge, Mass., 1971, pp. 321–328.

49. R. F. S. Hearmon, *An Introduction to Applied Anisotropic Elasticity*, Oxford University Press, 1961, pp. 42–43.

50. B. T. Kelly, *Mechanical Properties of Graphite*, The Pennsylvania State University Conference on the Scientific Base of Carbon Technology, University Park, Pennsylvania, March 20–24, 1972.

51. R. E. Taylor, D. E. Kline, and P. L. Walker, Jr., *Carbon*, **6**, 333 (1968).

52. J. E. Ashton, J. C. Halpin, and P. H. Petit, *Primer on Composite Materials*, Technomic Pub. Co., Stamford, Conn., 1969, p. 107.

Received December 7, 1972
Revised April 16, 1973